Exp Fluids (2009) 47:85–93
DOI 10.1007/s00348-009-0639-0

RESEARCH ARTICLE

Comparison of light transmission and reflection techniques to determine concentrations in flow tank experiments

Markus Konz · P. Ackerer · P. Huggenberger · C. Veit

Received: 20 May 2008 / Revised: 4 February 2009 / Accepted: 23 February 2009 / Published online: 10 March 2009

Abstract Transmissive and reflective intensity measurements for visual concentration determinations in 2D flow tank experiments were compared and evaluated for their applicability in the study of flow and transport phenomena. A density-dependent heterogeneous flow experiment was conducted and transmission and reflection images of the dyed saltwater plume were analyzed. A single light source and dark curtains forced the light to pass through the porous media only, thus facilitating the transmission measurements. The reflection images delivered a more homogeneous spatial illumination than the transmission images. Major perturbations of the transmission images were lens flare effects and light dispersion within the bead–water–Plexiglas system which smear the front of the plume. Based on the conducted evaluation of transmissive and reflective intensity measurements, the reflection data delivered more reliable intensity values to derive solute concentrations in intermediate scale flow tank experiments.

1 Introduction

Laboratory scale flow tank experiments are increasingly used to investigate flow and transport phenomena in porous media. In 2D experiments, spatial and temporal measurements of plume concentration distributions have been made by direct non-intrusive optical observations of dye tracers. The photometric technique is based on Lambert Beer's law assuming an exponential decline of light intensity with increasing dye concentration. The intensity can be measured as either light transmitted through the three-phase system consisting of glass beads, freshwater or dyed water and the Plexiglas panes, or the intensity values can be taken from reflected light. For both techniques, the relationship between intensity and concentration needs to be determined by calibration.

Most intermediate scale experiments used reflected light for image analysis (e.g. Schincariol et al. 1993; Oostrom et al. 1992; Swartz and Schwartz 1998; Wildenschild and Jensen 1999; Simmons et al. 2002; Rahman et al. 2005; McNeil et al. 2006; Goswami and Clement 2007; Konz et al. 2008, 2009). The reflection measurement can be conducted with non-transparent porous media material and with thick flow tanks that prevent light transmission. Image noise, fluctuations in brightness, and reflections from the surroundings can have a negative impact on the reflection measurements. Konz et al. (2008) showed the impact of lens flare effects on reflection intensity measurements in homogeneous porous media flow experiments. The flare effect artificially increases the intensity of dark regions because of light scattering within the lens system of the camera. This leads to an underestimation of concentrations.

The light transmission technique to measure emitted light from behind the flow tank opposite to the light source is normally used in micromodel experiments with thin flow tanks (e.g. Corapcioglu et al. 1997; Detwiler et al. 2000; Huang et al. 2002; Theodoropoulou et al. 2003; Jones and Smith 2005). An excellent literature review of transmission experiments and data processing techniques can be found

M. Konz (✉) · P. Huggenberger
Department of Environmental Sciences, Institute of Geology, Applied and Environmental Geology Group, University of Basel, Basel, Switzerland
e-mail: markus.konz@ifu.baug.ethz.ch

Present Address:
M. Konz
Institute of Environmental Engineering, ETH Zurich, Zurich, Switzerland

P. Ackerer · C. Veit
Mechanical Institute of Fluids and Solids, CNRS UMR 7507, Louis Pasteur University, Strasbourg, France

in Catania et al. (2008). Since only the transmitted light is recorded for concentration determination, reflections from the surroundings can be excluded. The use of transmission intensities has the advantage that migration effects are averaged over the width of the flow model. Therefore, possible 3D effects are less severe than with reflection data. However, light scattering within the system of glass beads, water and Plexiglas leads to light dispersion (Huang et al. 2002; Rezanezhad et al. 2006). This effect does not arise if reflection intensities were imaged to derive concentrations.

The aim of this study is to compare the light reflection and transmission techniques and evaluate their applicability to intermediate scale flow tank experiments with heterogeneous porous media. The comparison focuses on the impact of (1) illumination homogeneity, (2) lens flare effects, and (3) light dispersion within the flow tank, on the intensity measurements.

2 Materials and methods

2.1 Materials

2.1.1 Flow tank

The flow tank (internal dimensions: 158 cm length × 98 cm height × 4 cm depth) used for the experiments was constructed of 2 cm thick Plexiglas sheets (Fig. 1). Tension pins prevented deformation of the sidewalls of the tank allowing for maximum viewable area. The bottom of the tank had six openings (diameter 0.9 cm) and another nine openings each were placed at the sides of the flow tank. The openings could be connected either to a peristaltic pump or to reservoirs in order to meet the targeted boundary conditions.

2.1.2 Porous matrix

The tank was filled with two different glass bead types in order to achieve a heterogeneous porous media. The coarse beads had a diameter of 2–2.4 mm and the fine beads' diameter was between 0.5 and 0.7 mm. Figure 2 shows the heterogeneous packing of the tank with the block of fine beads in the center of the tank. The tank was packed under fully saturated conditions and the glass beads were poured into the tank in order to avoid air trapping. The de-ionized water used for the experiments was kept constant at 20°C in two 1,700 l freshwater reservoirs to prevent degassing in the porous media. Water temperature was measured in the outflow reservoir after it passed the tank and no relevant changes (±1.5°C for all experiments and calibration) were detected. Therefore, degassing due to temperature changes can widely be excluded. Further, no formation of air bubbles could be observed on the tank walls at any time. The two zones were divided by stainless steel emplacement dividers, which were removed once when the targeted height of the fine porous media block was reached.

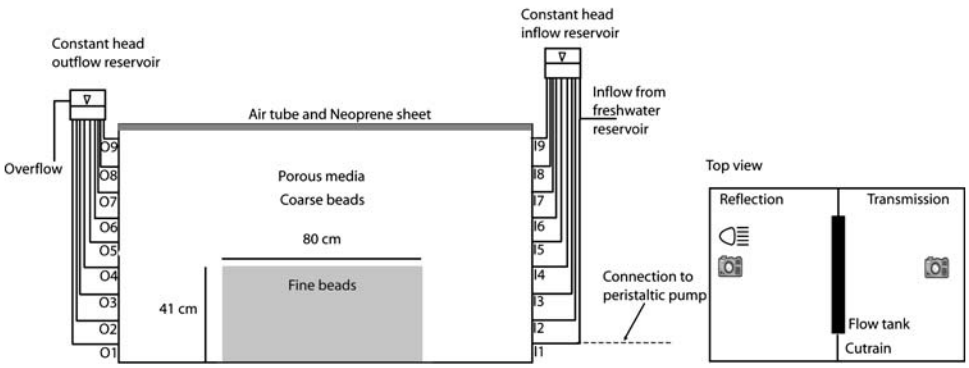

Fig. 1 Experimental flow tank

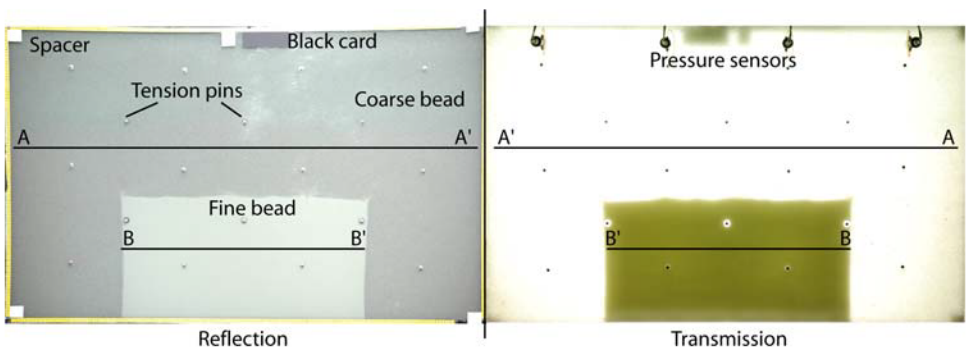

Fig. 2 Comparison of transmission and reflection images and position of profiles in Figs. 5 (AA′) and 12 (BB′)

2.1.3 Light source

A single light source was placed at a distance of 3 m away from the tank. The light source (Kobold-Licht, DFR200, 200 W, 5600 K) was adjusted and checked with a lux meter to minimize spatial lighting non-uniformity. However, it was not possible to avoid lighting non-uniformity and a higher intensity remained in the center of the image. The effects are discussed in Sect. 3.1 and shown in Fig. 5. Opaque, black curtains surrounded the entire tank. This setup forced the light to pass only through the porous media, a prerequisite for light transmission measurements.

2.1.4 Tracer

Cochineal Red A (E124) was used as tracer. This food dye is non-sorbing, non-reactive with NaCl in concentrations used for the experiment (Rahman et al. 2005 and our own batch experiments). The maximum absorption wavelength of the red dye is 507 nm. In order to test the tracer for degradation or optical decay of dye, the tank was filled with a dyed saltwater solution and images were taken over a period of 14 h. Intensity measurements were analyzed and revealed that the intensity values remained on a constant level. Additional photometric analyses using a spectrometer (Shimadzu UV-1700 Pharma Spec) to measure the intensities of different dye-saltwater solutions exposed to the same lighting proved that there is no degradation or optical decay of dye over a period of up to 7 days.

2.1.5 Camera

The images were recorded by two Nikon digital cameras (D70 and D80). The cameras deliver 12-bit images.

2.2 Methods

2.2.1 Image acquisition and image processing

Schincariol et al. (1993) and McNeil et al. (2006) outlined that the same image analysis techniques can be used for transmitted and reflected light. The image analysis method used here, is discussed in Konz et al. (2008) and the interested reader is referred to this publication for a detailed description of the image processing method. The procedure consists of: (1) data conversion to 16-bit tif images (65,536 intensity values per channel of the RGB color space) with the freeware dcraw (http://cybercom.net/~dcoffin/dcraw) to preserve the information of the 12-bit raw data, (2) selection of the most sensitive green channel (Konz et al. 2008; McNeil et al. 2006), (3) determination of measurement area (see Sect. 3.1), (4) correction of fluctuations in brightness using attached black cards, in the case of reflection measurements, (5) construction of a curve that relates intensities to concentrations from calibration images and determination of function parameters for the mathematical formulation of the curve expressed by:

$$C_{i,j}(t) = A1_{i,j}\exp\left(I_{i,j}^{\mathrm{corr}}(t)\Big/b1_{i,j}\right) + A2_{i,j}\exp\left(I_{i,j}^{corr}(t)\Big/b2_{i,j}\right) + D_{i,j} \quad (1)$$

where $C_{i,j}(t)$ is the concentration at time t, $A1_{i,j}$, $A2_{i,j}$, $D_{i,j}$, $b1_{i,j}$, $b2_{i,j}$, are parameters, $I_{i,j}^{\mathrm{corr}}$ is the brightness-corrected intensity at time t, and i and j are the coordinates of the pixels. The parameters have to be determined for each observation point in order to account for illumination heterogeneities (see Sect. 3.1).

2.2.2 Calibration and determination of appropriate camera settings

To establish the relationship between reflected/transmitted image intensity and salt concentration in Eq. 1, the entire tank was filled with solutions of predetermined saltwater–dye concentrations. The dyed saltwater solutions were pumped into the tank in a sequential order from low-density solutions to high-density solutions. Fifty images of transmission and reflection intensities were taken of each calibration solution to get a statistically significant measure of the dye intensities. The median of the 50 images was used to calculate the calibration intensity (Konz et al. 2008). Since concentration ranges from 0 to 100 g/l salt need to be resolved, 1 g/l dye concentration proves to be adequate to mark the maximum salt concentration of 100 g/l (Konz et al. 2008). The initial maximum dye concentration must be high enough so that, even with a large dilution, the plume can be differentiated optically from the ambient pore water. However, the maximum concentration needs to be below intensity saturation to enable the correct resolution of the high concentrations.

In order to find the appropriate camera settings, different parameter sets of shutter speed, aperture and ISO number were tested. The ability to resolve intensity differences between the 70 and 100 g/l solutions defines the adequate parameter set. Since the brightness differences between the two bead glasses are high, the parameter set used for the experiments represents a compromise to determine concentrations of both zones with one camera. The camera parameters must be constant and should not vary automatically so that the brightness corrected intensity variations can only be related to variations in dye concentration.

Figure 3 shows the calibration curves of intensity versus concentration for points in the fine and the coarse zone

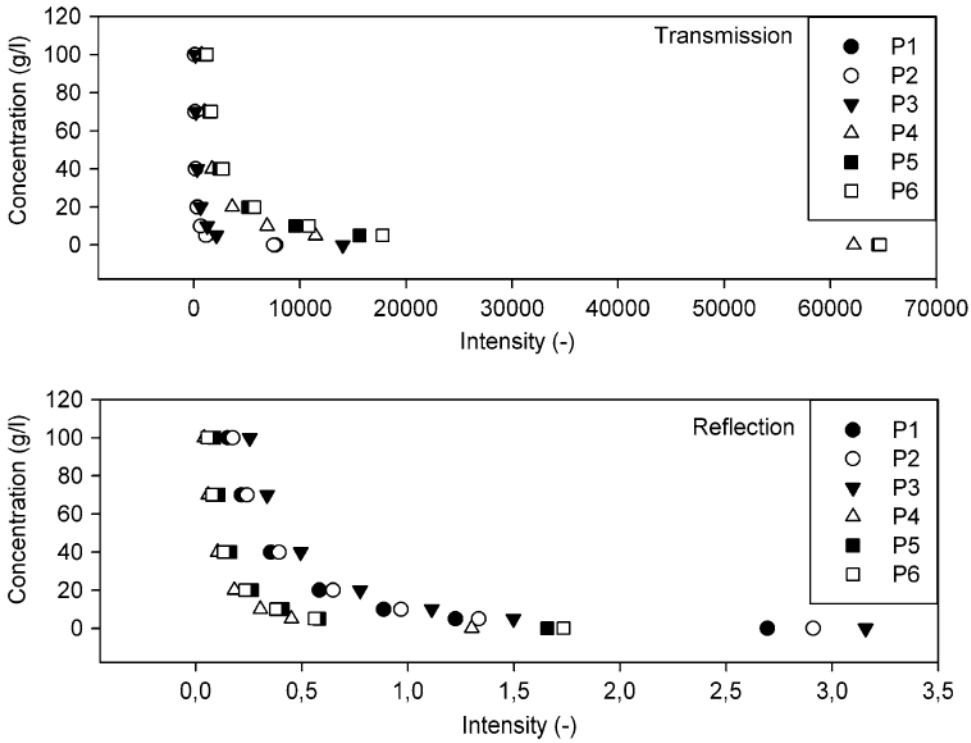

Fig. 3 Calibration curves for points of transmission and reflection images. *P1–P3* are placed in the fine beads, *P4–P6* in the coarse beads

using a shutter speed of 2 s, aperture of 4.5 and ISO200 for transmission and 1 s, aperture of 8 and ISO200 for reflection. The intensities of the reflection measurements are brightness corrected [see point (4)], therefore the values in Fig. 3 are smaller than the transmission data.

2.3 Experimental procedure

A density dependent flow experiment, E1, shows the applicability and limitations of the transmissive and reflective measurement techniques to derive concentrations of heterogeneous flow tank experiments. The flare effects in the camera lenses (Rogers 1976; Konz et al. 2008) and light dispersion due to scattering within the 3-phase system of beads, water/dye and Plexiglass (Huang et al. 2002; Rezanezhad et al. 2006) represent crucial perturbations of optical measurements. The experiments E2 and E4 were conducted in order to demonstrate the impact of these effects on intensity measurements in our experimental setup. Experiment E3 shows a possible way to minimize the effect of lens flare.

2.3.1 Density-driven flow experiment (E1)

The dyed solute of 100 g/l salt marked with 1 g/l dye was pumped into the domain through I1 and O8 was used as outlet (Fig. 1). Therefore, the tank continuously filled with solute and the bright region was reducing during the course of the experiment.

2.3.2 Assessment of lens flare effect (E2)

Three black cards were placed sequentially above each other at the transmissive side of the tank to reduce the bright region of the tank (Fig. 4). Images were taken from each step and the development of intensity profiles of the first card was observed.

2.3.3 Density-driven flow experiment with attached mask (E3)

A black mask with observation holes was attached on the transmissive side of the tank in order to reduce the flare

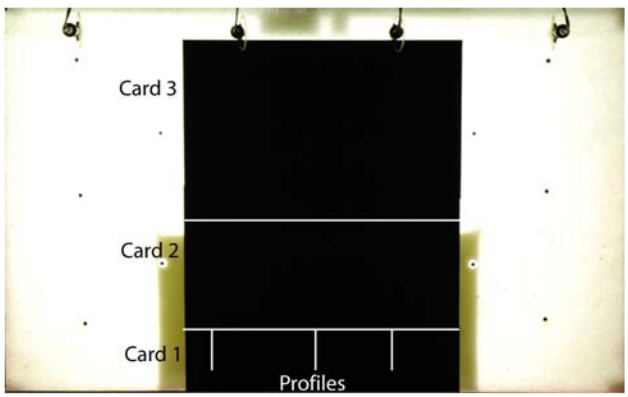

Fig. 4 Black card experiment, E2, to show the impact of lens flare effects on the intensity measurements along profiles of Card 1

effect. The same density dependent flow experiment as in E1 was conducted.

2.3.4 *Assessment of light dispersion effect (E4)*

The last experiment examined the light scattering in the 3-phase system. Three slits of 7–13 cm length (1–1.5 cm wide) in masks attached on the reflection side of the tank reduced the light source and the transmission images were recorded. The recorded transmission images should ideally deliver a sharply delineated slit. However, light is subject to reflection and refraction within the 3-phase system, resulting in light dispersion.

3 Results and discussion

3.1 Homogeneity of illumination and determination of measurement area

Figure 2 shows a reflection image and a transmission image. The fine glass bead is highly reflective and therefore appears brighter than the coarse beads on the reflection image. For the transmission, it is vice versa and the coarse bead zone transmits more light. The horizontal intensity profiles in Fig. 5 (AA′ in Fig. 2) indicate a brighter region in the center of the tank for both reflection and transmission measurements. The brightness variations along the reflection profile are less pronounced than along the transmission profile. Although the glass beads act as prism, spatial homogeneous illumination cannot be achieved by transmission measurements. However, this is not a disadvantage because the parameters of Eq. 1 are determined, for each observation point, specifically. Since the heterogeneous illumination-patterns are equal for each image and independent of the dye intensity of the experiments, the observation point based calibration accounts for illumination heterogeneity. Vignetting could also cause a reduction of an image's brightness or saturation at the periphery compared to the image center (Ray 2002). The calibration procedure accounts for that and avoids errors caused by vignetting.

The glass beads cause noise and the precision of point measurements increases with increasing number of pixels summarized to the observation point (Konz et al. 2008). The transmission images had a resolution of 0.46 mm per pixel, the reflection images had 0.56 mm per pixel. Two different cameras were used (Nikon D70 and D80), which explains the differences in resolution. Standard deviations (%) of intensities of eleven 100 × 100 pixel squares consisting of 10,000 pixels each, placed in the fine beads zone and in the coarse beads zone, were calculated in order to show the optical heterogeneity for transmission and reflection images (Fig. 6). The reflection measurements deliver higher deviations for the coarse beads of about 12% and about 4% for the fine beads. The transmission intensities show no differences between the bead sizes. In order to determine the appropriate measurement resolution, we

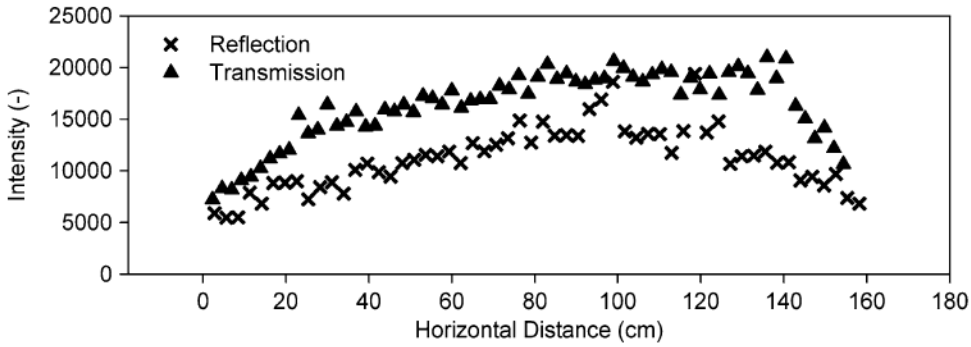

Fig. 5 Horizontal intensity profile AA′ (Fig. 2) for transmission and reflection intensities

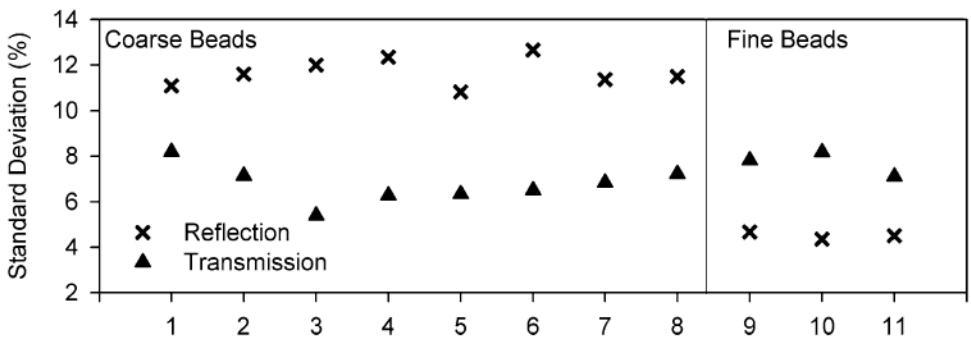

Fig. 6 Standard deviations of eleven 100 × 100 pixel squares

analyzed the intensity distributions in the 100 × 100 pixel squares. The intensities were determined by medians of stepwise increased pixels from 1 × 1 to 20 × 20 pixels. The standard deviation was taken as a measure for the quality of the calculated intensity value. The appropriate measurement resolution was found to be 10 × 10 pixels for transmission images and 10 × 10 pixels and 15 × 15 pixels for the fine, coarse beads of the reflection images, respectively. The reflection images are therefore more sensitive to the grain size than the transmission images.

3.2 Lens flare effect and scattered light

Figure 7 compares the concentrations of three points spread along the tank during experiment E1, determined by transmission (blue) and reflection (red) measurements. The reflection images deliver the expected S-type curve, which reach the maximum concentration of 100 g/l. However, the transmissive concentration curves show significant deviations from the S-type curve. The onset of concentration rise compares well between transmissive and reflective measurements, but the transmission data exhibit plateaus over several minutes and a second concentration ascent can be observed at the end of the experiment. The effect is more pronounced for the fine beads than for the coarse beads. The curves of the coarse beads show a continuous ascent of concentration. Since the experimental conditions are stable (saltwater below freshwater) fingering is not relevant. Two sources of errors can explain this behavior of the transmission curves: (1) lens flare effects, and (2) light dispersion due to scattering within the porous media.

3.2.1 Lens flare effect

Cameras contain lenses, which are comprised of several lens elements. Lens flare is caused by light, which reflects internally on lens elements any number of times (back and forth) before finally reaching the digital sensor. Thus, flare is technically caused by internal reflections. In order to become significant, it requires an intense light source. In flow tank experiments, the most intense image light source is the reflection or the transmission of regions not affected by the dyed solute. The dye absorbs light and therefore reduces the intensity. Due to the flare effects, regions of the tank with high dye concentrations, resulting in low reflected or transmitted intensity, might appear brighter. During the course of E1, the reflection intensity reaches the level of the expected intensity for the maximum dye concentration of the solute found in the calibration experiments (Fig. 8). Perturbations caused by flare are minor in this experimental setup for reflection measurements. Konz et al. (2008) reported a relatively small error of up to 3% caused by flare effects for reflection images. In their experimental setup, a homogeneous porous media with the fine glass beads (diameter: 0.6 mm) was used. As shown in Fig. 2, the fine glass beads reflect more light than the coarse beads and therefore might generate relevant flare effects if the entire tank is filled with these beads. The transmission data in Fig. 8, however, show a continuous decline of intensity in line with the decrease of bright regions of the tank. The coarse beads appear significantly brighter than the fine beads causing the flare effects. The reflected black card intensity (see Fig. 2) in Fig. 8 is on a constant level, which proves the existence of a constant

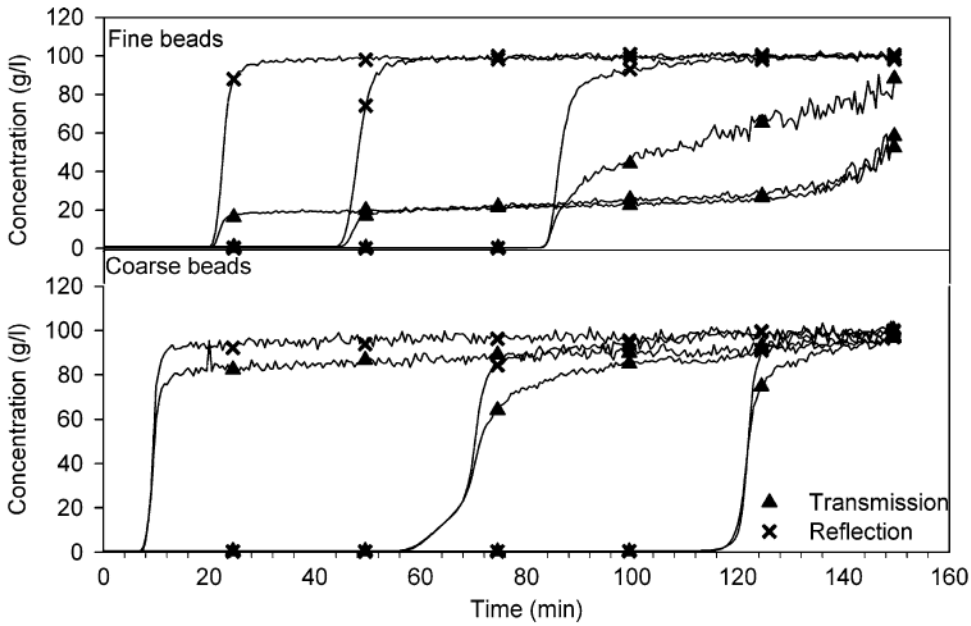

Fig. 7 Concentrations of E1 determined by reflection and transmission measurements

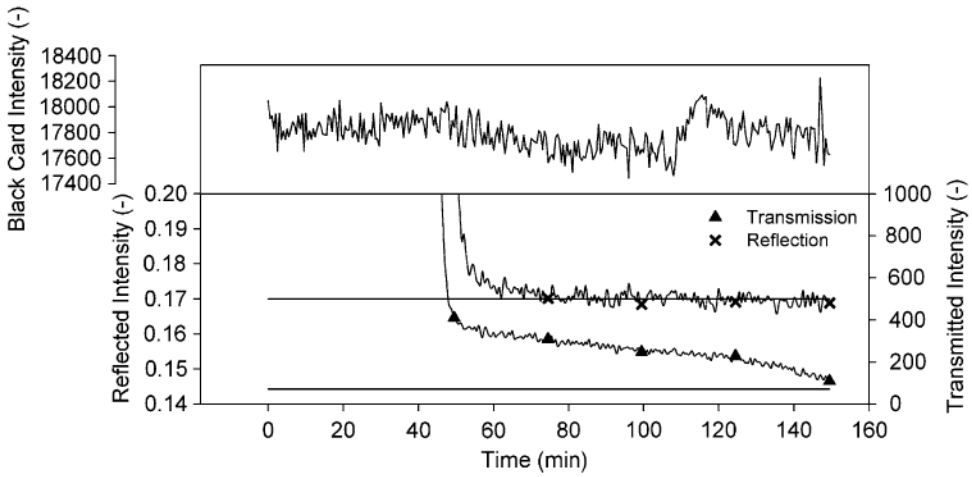

Fig. 8 Intensity values of reflection and transmission measurements with 100 g/l calibration intensity

light source. Therefore, changing illumination does not cause the decline of transmitted intensity. The impact of flare can also be observed by comparing the intensity of sequentially attached black cards on the transmission side of the tank (Konz et al. 2008). The profiles in Fig. 9 were taken from a 10 cm high black card placed at the bottom of the tank in E2 (Fig. 4). Additional black cards were attached in a sequential order and images were taken of each step. In the last step of E2, the cards covered the entire tank above the first card and therefore significantly reduced the transmitted light. Figure 9 shows the differences of intensities taken along profiles of the first card between the first and the last step. Up to 78% of intensity decline could be observed. A comparable experiment with reflection intensities delivered an error of less than 1%. Konz et al. (2008) showed that a black mask with observation holes could reduce the flare effect. In E3, a mask was placed on the transmission side of the tank with observation holes at different positions on the tank. The same density-dependent experiment as in E1 was conducted and intensity values were recorded at the observation holes. Figure 10 exemplifies the intensity developments for observation points in the fine beads zone and in the coarse beads zone. In contrast to E1 without the mask, the transmissive intensities reached a constant level during the course of E3 and no flare effects were observed (Fig. 10). The mask significantly reduced the light of the transmission image and thus eliminated the prerequisite for flare effects. The experiments E2 and E3 showed the relevance of this effect for transmission measurements.

3.2.2 *Light scattering*

Scattering within the bead–water–Plexiglas system causes light dispersion of the transmission image smearing the plume front (Huang et al. 2002; Rezanezhad et al. 2006). The dispersion of light intensity is shown for one slit of E4 in Fig. 11. The 1.5 cm wide slit causes an area with an extent of up to 27 cm to be affected. The center of the affected area matches with the location of the actual edges of the silts. The coarse glass beads favor the Gaussian-like decay of intensity due to light dispersion, whereas the effect is less pronounced for the fine beads. Scattering reduces the contrast between zones of different dye

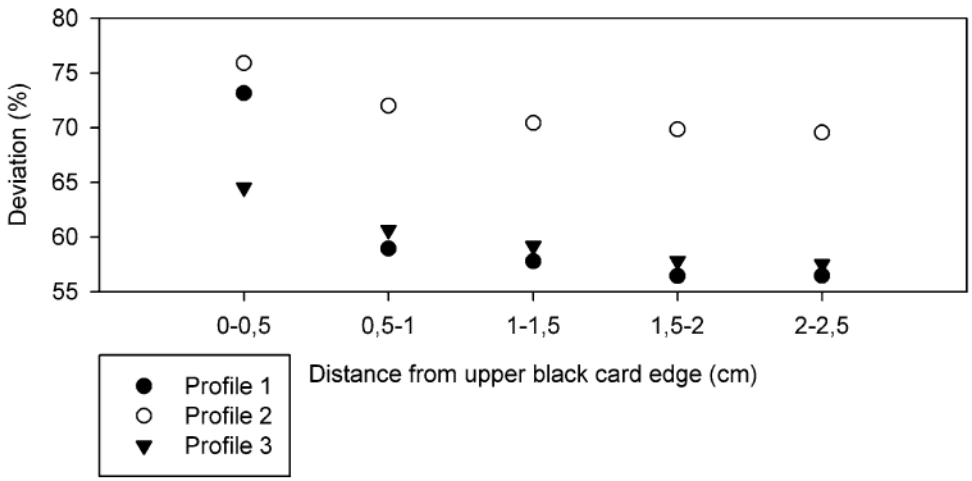

Fig. 9 Intensity deviation (%) between the first and the third step of E2 along vertical profiles of black Card 1 shown in Fig. 4

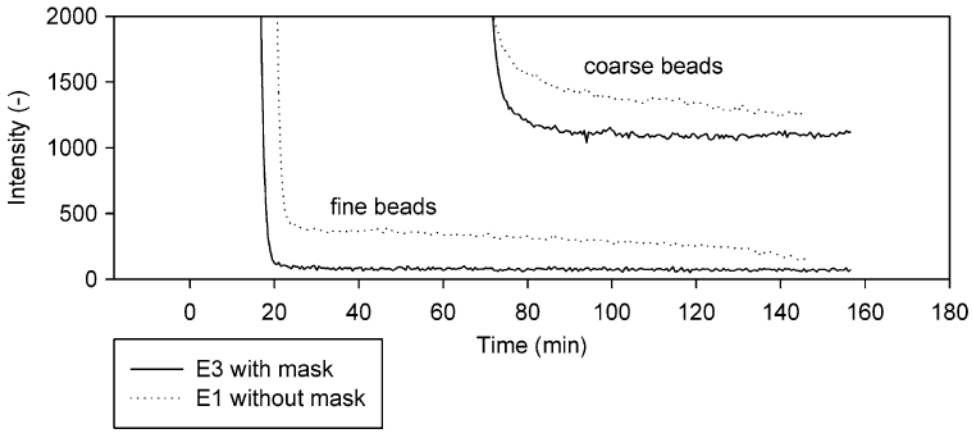

Fig. 10 Comparison of transmission intensities of E1 without the mask and E3 with the mask

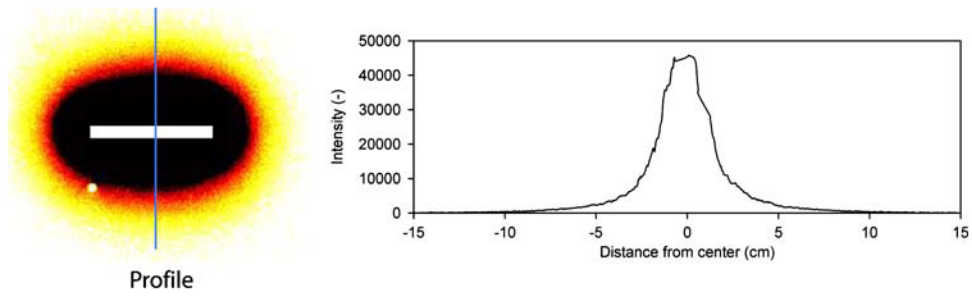

Fig. 11 Light dispersion caused by a rectangular slit (*white*). The intensities are taken along the vertical profile

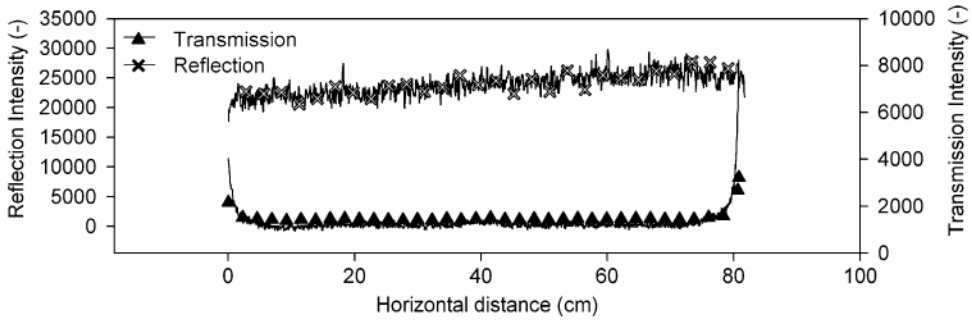

Fig. 12 Horizontal reflection and transmission intensity profiles, BB′ (Fig. 2) along the fine glass beads

concentration and between porous media classes, and therefore smears the front of the plume. The profile BB′ (Fig. 2) in Fig. 12 shows an intensity increase at the edges of the fine glass bead zone caused by scattered light from the coarse beads zone. This effect can be observed for 0 and 1 g/l (100 g/l salt concentration) of dye concentration. Rezanezhad et al. (2006) applied a point spread function to correct for distortion of the images. Their results proved the ability of the procedure to improve the images. However, the effect still has an impact on the quality of the transmission data. The effect also depends on the width of the tank and is therefore reduced in thin flow tanks.

4 Conclusions

We compared transmission and reflection intensity measurements to determine solute concentrations in heterogeneous intermediate scale laboratory experiments using an ordinary light source and a non-fluorescent dye tracer. This was done regarding illumination homogeneity of the photographed domain, lens flare effects and scattered light within the bead–water–Plexiglas system. The following phenomena could be observed:

- Fine glass beads appear brighter than coarse beads on the reflection image and vice versa on the transmission image.
- The reflection images deliver a more homogeneous spatial illumination than the transmission images.
- The noise from the glass beads is the most pronounced at the coarse beads of the reflection images.
- Lens flare effects significantly perturb the transmission measurements.
- Scattered light within the bead–water–Plexiglas system smears the plume front of the transmission images.

Due to these phenomena, the light reflection method outperformed the transmission method in our experimental setup. The perturbations are highly dependent on the experimental setup, e.g. width of the tank, camera and light source position. It is therefore recommended to assess the perturbations of the intensity measurements for each setup specifically. The mask with observation holes reduces the flare effect; however, it also reduces the data availability to a predefined number of observation points and does not allow for the determination of concentration contour lines. The utilization of fluorescent dye under ultra-violet illumination could reduce the lens flare effect since the light captured by the camera is emitted from the tracer itself.

Acknowledgments The authors are grateful to Dr. Lukas Rosenthaler of the Imaging and Media Lab, University of Basel who contributed significantly to the image analysis method. Further, we acknowledge the valuable comments of three anonymous referees. This study was financed by the Schweizer Nationalfond 200020-109200.

References

Catania F, Massabo M, Valle M, Bracco G, Paladino O (2008) Assessment of quantitative imaging of contaminant distributions in porous media. Exp Fluids 44:167–177

Corapcioglu MY, Chowdhury S, Roosevelt SE (1997) Micromodel visualization and quantification of solute transport in porous media. Water Resour Res 33(11):2547–2558

Detwiler RL, Rajaram H, Glass RJ (2000) Solute transport in variable-aperture fractures: an investigation of the relative importance of Taylor dispersion and macrodispersion. Water Resour Res 36(7):1611–1625

Goswami R, Clement P (2007) Laboratory-scale investigation of saltwater intrusion dynamics. Water Resour Res 43:W04418

Huang W, Smith CC, Lerner DN, Thornton SF, Oram A (2002) Physical modelling of solute transport in porous media: evaluation of an imaging technique using UV excited fluorescent dye. Water Res 3(7):1843–1853

Jones EH, Smith CC (2005) Non-equilibrium partitioning tracer transport in porous media: 2-D physical modelling and imaging using a partitioning fluorescent dye. Water Res 39(20):5099–5111

Konz M, Ackerer P, Meier E, Huggenberger P, Zechner E, Gechter D (2008) On the measurement of solute concentrations in 2-D flow tank experiments. Hydrol Earth Syst Sci 12:727–738

Konz M, Ackerer P, Younes A, Huggenberger P, Zechner E (2009) 2D Stable layered laboratory-scale experiments for testing density-coupled flow models. Water Resour Res 45:W02404. doi:10.1029/2008WR007118

McNeil JD, Oldenborger GA, Schincariol RA (2006) Quantitative imaging of contaminant distributions in heterogeneous porous media laboratory experiments. J Contam Hydrol 84:36–54

Oostrom M, Dane JH, Guven O, Hayworth JS (1992) Experimental investigation of dense solute plumes in an unconfined aquifer model. Water Resour Res 28:2315–2326

Rahman A, Jose S, Nowak W, Cirpka O (2005) Experiments on vertical transverse mixing in a large-scale heterogeneous model aquifer. J Contam Hydrol 80:130–148

Ray SF (2002) Applied photographic optics, 3rd edn. Focal Press

Rezanezhad F, Vogel HJ, Roth K (2006) Experimental study of fingering flow through initially dry sand. Hydrol Earth Syst Sci Discuss 3:2595–2620

Rogers G (1976) Photography in paediatrics. In: Newman A (ed) Photographic techniques in scientific research, vol 2. Academic Press, ISBN 0 12 517960

Schincariol RA, Herderick EE, Schwartz FW (1993) On the application of image analysis to determine concentration distributions in laboratory experiments. J Contam Hydrol 12:197–215

Simmons CT, Pierini ML, Hutson JL (2002) Laboratory investigation of variable-density flow and solute transport in unsaturated–saturated porous media. Transp Porous Media 47:15–244

Swartz CH, Schwartz FW (1998) An experimental study of mixing and instability development in variable-density systems. J Contam Hydrol 34:169–189

Theodoropoulou MA, Karoutsos V, Kaspiris C, Tsakiroglou CD (2003) A new visualization technique for the study of solute dispersion in model porous media. J Hydrol 27(1–4):176–197

Wildenschild D, Jensen KH (1999) Laboratory investigations of effective flow behavior in unsaturated heterogeneous sands. Water Resour Res 35:17–27